Full Length Article

Autoignition of sustainable fuels under dual operation with H_2-carriers in a constant volume combustion chamber

Juan J. Hernández [a],[*], A. Cova-Bonillo [a], A. Ramos [a], H. Wu [b], J. Rodríguez-Fernández [a]

[a] *Universidad de Castilla-La Mancha, Escuela Técnica Superior de Ingeniería Industrial, Avda. Camilo José Cela s/n., 13071 Ciudad Real, Spain*
[b] *School of Mechanical Engineering, Beijing Institute of Technology (BIT), Beijing 100081, China*

ARTICLE INFO

ABSTRACT

The expected increase in the use of environmentally friendly liquid fuels in medium and heavy-duty compression ignition engines (for both off-road and transport applications), together with the well-documented benefits of hydrogen-carriers to decrease energy dependence and to achieve a neutral-carbon economy (internal combustion engines highly contributing to the global CO_2 emissions), have motivated this work. The autoignition characteristics of different alternative diesel-type fuels (hydrotreated vegetable oil, advanced biodiesel and blends of conventional diesel fuel with polyoxymethylene dimethyl ether and 1-butanol) under dual-fuel operation with H_2, NH_3, and CH_4 were studied in a constant volume combustion chamber at 535 and 600 °C. The high reactivity fuel was replaced by the gaseous fuel up to 40 % by energy. The main ignition delay time was significantly affected not only by the type of low reactivity fuel, with ammonia considerably retarding autoignition, but also by the nature of the liquid fuel, biodiesel being the less sensitive to the presence of the H_2-carrier fuel. Results also proved that the higher the reactivity of the diesel-type fuel (quantified through the cetane number), the lower the influence of the gaseous fuel on the autoignition time.

1. Introduction

Compared to a bi-fuel internal combustion engine, for which two fuels are burnt separately, a compression ignition dual-fuel configuration refers to an engine that runs on two fuels simultaneously [1]. One of them is typically a highly reactive, diesel-like fuel used as an igniter, and it usually accounts for as little as 5–10 % of the in-cylinder energy in commercial propulsion systems. The other typically has a low autoignition tendency and provides most of the energy released in combustion [2]. One of the main benefits of the dual-fuel mode is the partial replacement of fossil diesel fuel by an alternative fuel with lower CO_2 life-cycle emissions and/or renewable origin. Although electrification of light duty vehicles has been recognized as the strategy to line a CO2-neutral transportation sector, performance limitations of batteries (energy density and price) are expected to delay the transition away from combustion engines regarding heavy-duty applications [3], for which compression ignition (CI) engines are the dominant propulsion source. Given this scenario, dual-fuel operation could provide significant decreases in CO2 life-cycle emissions for applications that will continue to be highly carbon intensive in the short-medium term. Regarding the way of feeding both fuels in dual CI engines, the high reactivity-one (HRF)

uses to be directly injected (DI) while the low reactivity fuel (LRF) can be port (PFI) or directly injected, the latter either separately or together with the HRF through a dual-fuel injector [4]. The first option is the most cost-effective since it does not require significant modifications on the original engine structure and settings, thus accelerating the transition to a more sustainable internal combustion engine fleet (both for mobility and off-road applications). The relatively recent "reactivity-controlled compression ignition (RCCI)" concept is just an example of dual-fuel combustion which targets for ultra-low NOx and soot emissions while maintaining good fuel economy [5].

Among the typical LRFs used under CI dual-fuel mode, natural gas has been the most widely tested because of its abundance, low specific CO_2 emissions, and a relatively clean combustion [4,6]. Performance and pollutant emissions of CI engines with hydrogen addition have also been widely reported [7,8], even combined with natural gas since the properties of hydrogen (extremely high combustion speed, very wide flammability limits and a very short flame quenching distance) reduces methane slipping and thus the subsequent problems derived from the global warming potential of this compound [9]. Because of the recent interest of H_2-derived fuels (such as the so-called e-fuels, mainly light alcohols), other sustainable compounds are being currently evaluated, ammonia having interest not only because of its higher energy density

---

* Corresponding author.
E-mail address: JuanJose.Hernandez@uclm.es (J.J. Hernández).

Nomenclature

ASTM	American Society for Testing and Materials
BDE	Bond Dissociation Energy
CF	Cool flame
CN	Cetane Number
CVCC	Constant Volume Combustion Chamber
DCN	Derived Cetane Number
E_{LRF}	Energy replacement (%) with the low reactivity fuel
Fr	Equivalence fuel/air ratio
HRF	High Reactivity Fuel
ID_{CF}	Ignition delay for the cool flame, ms
ID_M	Main ignition delay, ms
LHV	Lower Heating Value, MJ/kg
LRF	Low Reactivity Fuel
p	Pressure, bar
p_0	Initial Pressure, bar

PFI	Port Fuel Injection
RCCI	Reactivity-Controlled Compression Ignition
T	Temperature, °C
T_0	Initial Temperature, °C
$dp/dt_{max,}$	maximum pressure gradient, bar/ms

Chemical compounds:

2-EHN	2-ethylhexyl nitrate
Bu20D	blend of 80 % diesel fuel and 20 % 1-butanol (by vol.)
$Bu20D_i$	Bu20D blended with 2-EHN (1 % by vol.)
CH_4	methane
$Diesel_i$	Diesel blended with 2-EHN (1 % by vol.)
HVO	Hydrotreated Vegetable Oil
H_2	hydrogen
NH_3	ammonia
OME	Polyoxymethylene Dimethyl Ethers
OME20D	blend of 80 % diesel fuel and 20 % OME_{3-5} (by vol.)

---

when compared to hydrogen but also because it has no direct-CO_2 emissions and the worldwide availability of distribution infrastructure [10,11]. However, and due to the huge autoignition resistance of ammonia, works dealing with this fuel are mainly focused on spark ignition engines [12].

Regarding the high reactivity fuel, although conventional diesel fuel is the most common, biodiesel and diesel/biodiesel blends have also been studied [13,14] since biodiesel is currently present in commercial diesel fuels, as mandatory by the EU directive EU/2018/2001 [15]. Hydrotreated vegetable oil (HVO), which can be produced by catalytic hydrogenation of wastes and residues, is postulated as the most promising alternative for fossil diesel because of its outstanding properties as a drop-in CI fuel (autoignition reactivity, absence of aromatics compounds and superior cold flow behaviour) [16]. There has been some controversy regarding its sustainability since it has depended on the raw vegetable oil, which competes with food production as well as the production cost of the HVO. However, currently waste and residues represent over 80 % of the HVO raw materials input and the greenhouse gas reduction can be up to 90 % compared to fossil diesel. Also the production cost of HVO is not significantly higher compared to crude oil based production. Moreover, HVO has potential to greatly reduce particle mass emissions (up to 9 % in some cases) when compared to diesel fuel, as shown in a recent review from Szeto and Leung [17].

Polyoxymethylene dimethyl ethers (usually denoted OMEx), have emerged in the last years as potential substitutes of diesel fuel because of their renewable origin and some superior characteristics, mainly their noticeable oxygen content and the absence of C—C bonds (which positively affect soot emissions [18]), as well as their great cetane number [19,20]. Their general chemical formula is $CH_3O–(CH_2O)_n$-CH_3, where n usually ranges from 1 to 6 [21]. Unlike other oxygenated fuels (such as dimethyl ether or methanol), with a higher toxicity and vapour pressure at room temperature, OMEx is a non-toxic and colourless liquid fuel. However, because of its poor heating value and cold flow behaviour, OMEx cannot be used as pure but as a diesel blendstock in practical applications [22,23].

Against ethanol, 1-butanol is a much more suitable bio-alcohol to be blended with diesel fuel because of its widely documented better properties (i.e., miscibility, heating value and cetane number) [24]. It can be produced either by sustainable catalytic processes based on ethanol [25] or through the biological conversion of biomass/wastes with the bacteria Clostridium Acetobutylicum (Acetone-Butanol-Ethanol (ABE) process) [26]. However, the 1-butanol content in blends with diesel has still to be limited (up to around 20 % by volume [24]) to avoid, among others, deteriorated combustion processes derived from a very delayed start of combustion mainly under cold start conditions.

As well known, autoignition is a key phenomenon governing performances and pollutant emissions of CI engines. Despite some works can be found in literature describing the effect of different low reactivity fuels on the ignition of diesel-type fuels, most of them are focused on natural gas and hydrogen as LRF and on conventional diesel or biodiesel as HRF, as mentioned before. From the best of the authors' knowledge, the base fuel-dependent effect of the LRF on the autoignition phenomena has not been yet analysed. Not only the type of LRF but also the reactivity and the chemical structure of the HRF could influence the ignition delay time, thus advising towards modifications on the injection strategy to compensate possible shifts on the combustion phasing. Moreover, few of the published works have been carried out in well-controlled devices (shock tubes, rapid compression machines, constant volume combustion chambers) allowing for isolating the effect of the fuel from other phenomena (turbulence, temperature yield, etc.) caused by compression and heat transfer, the latter being important in engines. Considering the previously mentioned comments, the low-intermediate autoignition behaviour of several promising diesel-type fuels (biodiesel, HVO and OME_{3-5}) under dual mode with three H_2-derived gaseous fuels (H_2, NH_3 and CH_4) has been experimentally analysed in a constant volume combustion chamber (CVCC). Energy replacements of the diesel-type fuel with the LRF up to 40 % have been checked at two temperatures (535 and 600 °C). Results will provide fundamental understanding on the HRF-dependent effect of using H_2-derived fuels under dual fuel CI operation and they can also support the optimization of the engine settings under a scenario in which sustainable diesel-type fuels will play a much more important role.

2. Fuels and experimental setup

2.1. Fuels

Three pure fuels and two blends were used as HRFs. Diesel fuel, supplied by Repsol (Spain), was tested as reference. Unlike commercial fuels supplied in filling stations, it was an oxygen-free fuel to clearly distinguish it from other of the fuels tested (biodiesel). Biodiesel, provided by the company Bio Oils (Spain), was produced from soybean and palm oils. It mainly consisted of (by mass) 47.26 % methyl linoleate (C18:2), 26.22 % methyl oleate (C18:1), 15.62 % methyl palmitate (C16:0), 5.39 % methyl α-linolenate (C18:3) and 3.77 % methyl stearate (C18:0). Lastly, hydrotreated vegetable oil (HVO), supplied by Neste (Finland), with an isoalkane/*n*-alkane ratio of about 1.12, was the most reactive HRF. Regarding the blends, OME20D denotes a blend of diesel fuel and OME_{3-5} (80/20 % by vol.), while Bu20D refers to a blend between the reference fuel and 1-butanol (also 80/20 % by vol.). The OME

Table 1
Properties of the fuels tested.

Property	Method	Diesel	Biodiesel	HVO	OME$_{3-5}$	OME20D	Bu20D	H$_2$	NH$_3$	CH$_4$
C (% m/m)	EN ISO 16,948	86.4 [a]	77.1	84.7	44.7	76.8	82.2	~	~	74.9
H (% m/m)	EN ISO 16,948	13.5 [a]	11.9	15.3	9.0	12.3	13.6	100	17.8	25.1
O (% m/m)	EN ISO 16,948	0 [a]	11.0	0	46.3	10.9	4.3	~	~	~
N (% m/m)	~	~	~	~	~	~	~	~	82.24	~
Density$_{15°C}$ (kg/m^3)	EN ISO 3675	842.0 [a]	883.5	779.3	1058	885.7	823.3	~	~	~
Surface tension$_{20°C}$ (mN/m)		27.9	31.4	~	~	~	~	~	~	~
Kinematic viscosity$_{40°C}$ (cSt)	EN ISO 3104	2.39	4.19	2.93	1.09	~	~	~	~	~
Lower heating value (MJ/kg)	UNE 51,123	42.90 [a]	37.64	43.81	19.36	37.22	40.99	120.0 [b]	18.80 [b]	50.00 [b]
Derived cetane number	ASTM D7668	52.0 [a]	52.5	80.1	69.4	53.1	46.0	~	~	~
Stoichiometric fuel/air ratio	N/A	1/14.50	1/12.50	1/14.95	1/6.23	1/12.45	1/13.84	1/34.33	1/6.05	1/17.41
Molecular weight (kg/kmol)	N/A	203.08	291.26	221.67	152.54	191.50	150.97	2.02	17.03	16.04
H/C ratio	N/A	1.83	1.85	2.15	2.41	1.91		~	~	~
Autoignition temperature (K) [c]	~	503	~	~	~	~	~	844	924	723
Laminar burning velocity (m/s) [c]	~	~	~	~	~	~	~	2.91	0.07	0.37

[a] Measured.
[b] Taken from NIST Chemistry WebBook[30].
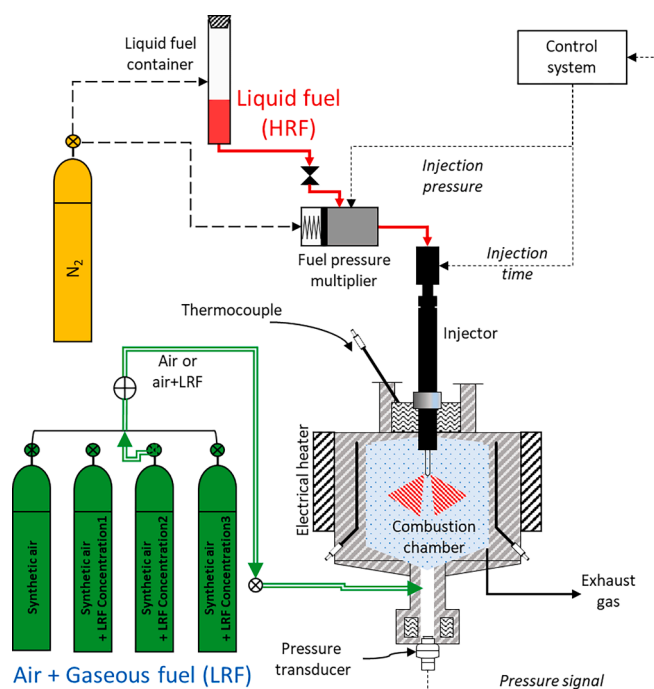[c] Taken from Chai et al.[31].

Fig. 1. Scheme of the experimental setup.

content in the blend with the reference diesel fuel was selected from works proving this ratio as optimum considering both engine pollutant emissions [27,28] and cold flow properties [23]. OME consisted of OME$_{1-2}$ < 0.01 %; OME$_3$ = 57.24 %; OME$_4$ = 28.49 %; OME$_5$ = 10.61 % and OME$_6$ = 2.34 % (by weight). Besides, 20 % of 1-butanol has been reported as a limit to avoid operational problems mainly related to cold start conditions [24,29].

In addition, methane (CH$_4$), ammonia (NH$_3$) and hydrogen (H$_2$) were used as LRFs. Synthetic bottles containing air mixed with each of these gases were used in the constant volume combustion chamber. The concentration of the gases was that matching the desired HRF energy replacement (10, 20 and 40 %). Table 1 shows the main properties of all the fuels considered.

2.2. Experimental procedure

The experimental tests were performed as described by Hernández et al. in [32]. The device was a Cetane ID510 constant volume combustion chamber (CVCC) by Herzog (complying with the ASTM D7668 standard [33]). Fig. 1 shows a general scheme of the set-up. Having a volume of 0.473 L, it is equipped with a common-rail diesel injector which allows for both changing the injection pressure (1000 bar was chosen for this work) and the injection duration (between 400 and 3000 µs). The initial chamber temperature (T_0) and pressure (p_0) can be ranged from 535 to 650 °C and from 1 to 30 bar, respectively (this latter parameter was maintained at 21 bar in this work). Two different temperatures were tested (535 and 600 °C) to check the role of the LRF depending on the reaction routes governing the oxidation of the diesel-type fuel (HRF). Before testing a new fuel, two flushes of the chamber by using this new fuel were carried out to remove any residue from the previous one. Moreover, prior to the fifteen injections used for determining the ignition delay time, the system carries out five injections to further eliminate wastes from previous tests. The raw results are obtained in terms of pressure versus time records. These were processed by means of the diagnostic model described in [34].

The main indicators of the autoignition behaviour were the delay times. For this purpose, the criteria proposed by Lapuerta et al. [35] was adopted. Thus, the cool flame delay time (ID_{CF}) was the time elapsed from the start of injection to the instant when the pressure rises 0.2 bar above the initial pressure (subject to the appearance of two stages in the dp/dt curves). The main autoignition delay time (ID_M) was identified as the instant at which the line joining 1/2 and 1/4 of the maximum pressure rate (dp/dt_{max}) equals zero. In the case where autoignition involves only one stage, the ignition delay was defned as the ID_M discussed above.

The experiments were carried for energy substitution ratios of around 10, 20 and 40 %, this ratio being calculated as shown in Eq. (1), where m_{LRF} and m_{HRF} are the mass of the gaseous and liquid fuel, respectively, and LHV_{LRF} and LHV_{HRF} are the corresponding lower heating values. For safety constraints, the supplier was not able to provide synthetic bottles of the H$_2$/air mixture allowing for the highest replacement (40 % by energy).

$$E_{LRF}(\%) = 100 \cdot \frac{m_{LRF} \cdot LHV_{LRF}}{m_{LRF} \cdot LHV_{LRF} + m_{HRF} \cdot LHV_{HRF}} \tag{1}$$

The experimental schedule was designed for keeping a similar energy input when changing either the LRF or the HRF (see Tables provided as supplementary material), trying to simulate similar conditions (brake power) in a practical engine. As also shown in those tables, the equivalence ratio (*Fr*, defined as the fuel/air ratio with respect to the stoichiometric one), which significantly affects the ignition delay, kept almost constant (between 0.35 and 0.40). The slight deviations observed for a same HRF/LRF pair are related to changes in the chamber temperature (which influences the amount of air/gas mixture introduced in
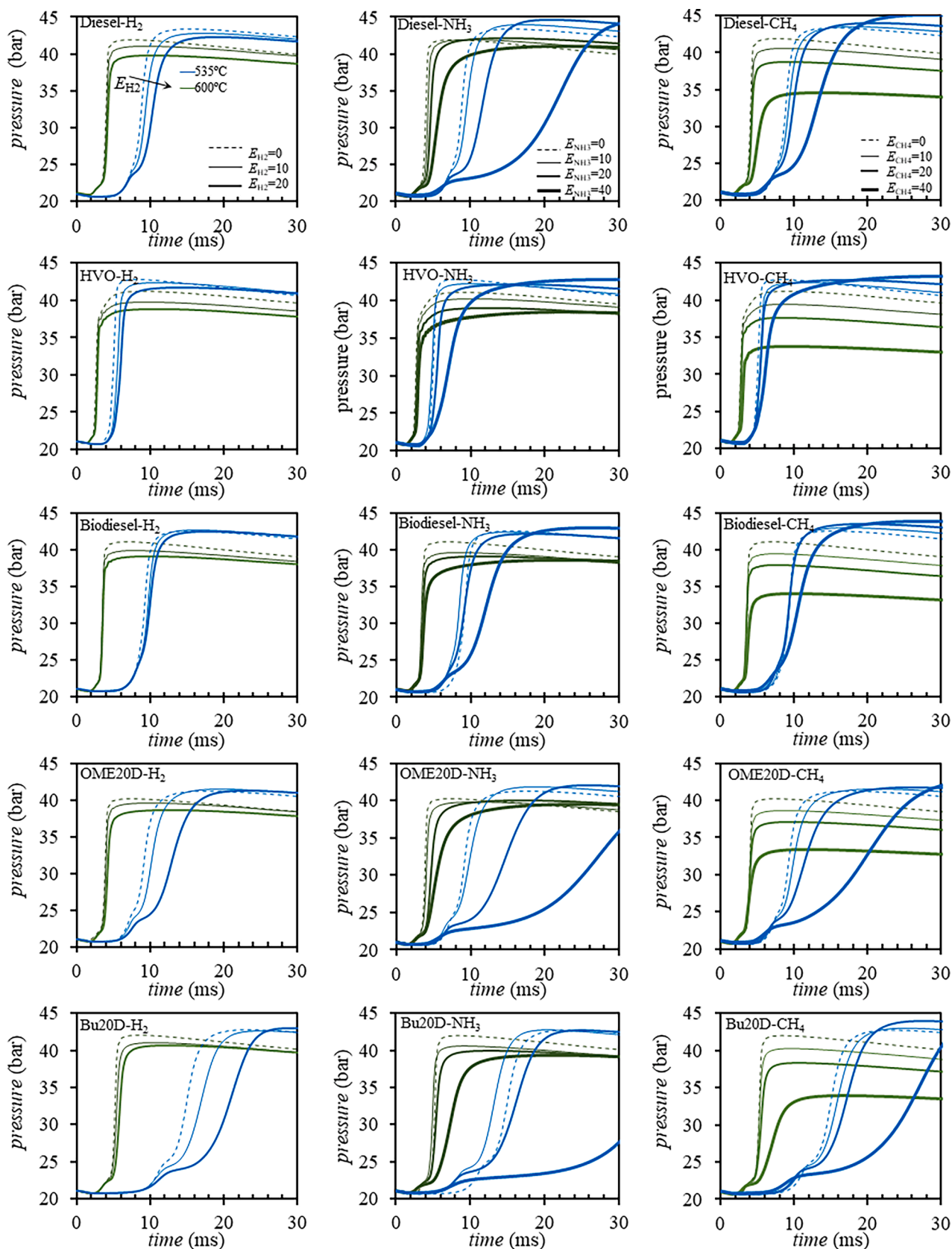
Fig. 2. Pressure traces for different replacements of diesel, HVO, biodiesel, OME20D and Bu20D with H_2 (left), NH_3 (center), and CH_4 (right) at $p_0 = 21$ bar and $T_0 = 535\ °C$ (blue) and $600\ °C$ (green). (For interpretation of the references to color in this figure legend, the reader is referred to the web version of this article.)
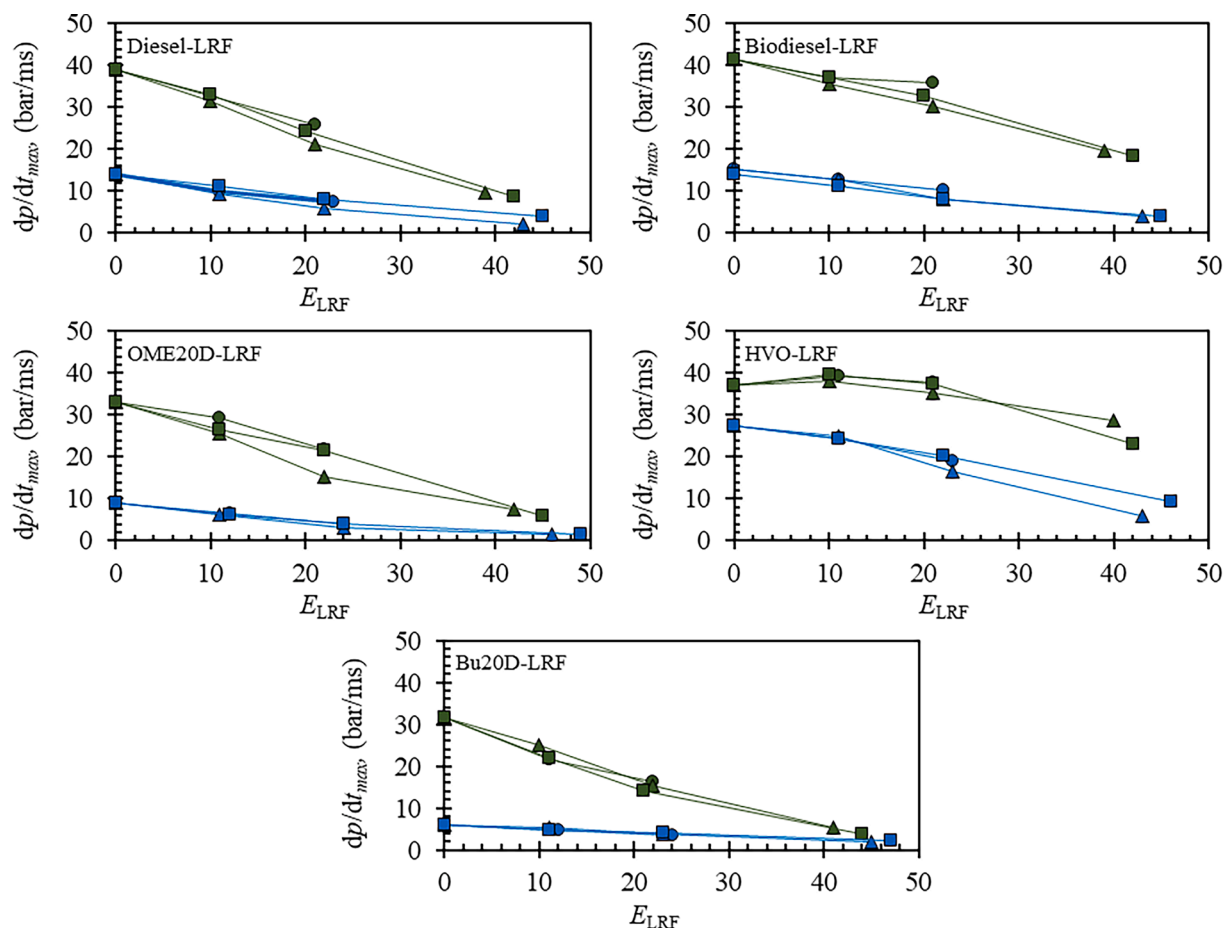
Fig. 3. Maximum pressure gradient for different replacements with H_2 (●), NH_3 (▲) and CH_4 (■) at $p_0 = 21$ bar and $T_0 = 535$ (blue) and 600 °C (green). (For interpretation of the references to color in this figure legend, the reader is referred to the web version of this article.)

the CVCC).

Additionally, to identify the differential effect of the LRF depending on the reactivity of the diesel-type fuel (HRF), additional tests were carried out by doping some of the fuels commented with a cetane improver. These fuels were the reference base fuel and Bu20D, the improved fuels denoted as "Diesel$_i$" and "Bu20D$_i$". The former was used to elucidate the role of the cetane number on autoignition while comparing fuels with a similar chemical structure (Diesel, Diesel$_i$ and HVO). Besides, Bu20D$_i$ was used to analyse the effect of the chemical structure while keeping a similar cetane number, for which Bu20D$_i$, Diesel, Biodiesel and OME20D were compared. The widely used 2-ethyl-hexyl nitrate (2-EHN) was chosen as ignition enhancer [36]. The amount of 2-EHN was based on the work by Kuszewski [37], who suggested that 10000 ppm (1 %) of 2-EHN leads to a CN enhancement of about 10 units. In this sense, an improved diesel fuel and Bu20D with a DCN of 63.2 and 51.2, respectively (measured according to ASTM D7668) were obtained. As reported by Ghosh [36], the way the CN enhancer works is by an early generation of $NO_2^\bullet$ radicals, which are more active than molecular oxygen (the only reactant available at the start of the autoignition) for initiating the oxidation process. No changes on the dominant kinetics pathways of the HRF are expected when adding 2-EHN, which guarantee the reliability of the conclusions obtained.

3. Results and discussion

The tested conditions (T_0, p_0, and *Fr*) and the resulting ID_{CF}, ID_M, peak pressure (p_{max}) and maximum pressure gradient (dp/dt_{max}) are shown in Tables SM1 to SM7 (supplementary material). The 95 % confidence limit values according to Student's *t*-distribution based on

the 15 cycles recorded for each test were also included. As observed, these values are much lower than the differences on the mean ignition delay times caused either by the fuel or by the operating conditions, which guarantee the significance of the trends discussed in this section. The pressure traces for the original high reactivity fuels are shown in Fig. 2 (green color for 600 °C and blue color for 535 °C). The thickness of each line indicates the proportion of LRF replacing the diesel-type fuel (E_{LRF}), the higher the substitution the thicker the line. The pure HRF was drawn by dashed lines.

As observed, a typical two-stage combustion process (low and high temperature heat release) occurred for all the conditions, as expected because of the long C-chain of the liquid fuels tested. An increase in E_{LRF} caused the main ignition to be delayed, while the occurrence of the cool flame seems to not be affected neither by the amount nor by the type of LRF. The longer ignition duration for increasing LRF replacements also led to leaner local equivalence ratios when ignition occurs, thus slowing down the combustion process, as shown by the slope of the dp/dt curves (Fig. 3 and supplementary material). This is more evident at 535 °C and for ammonia, since the combustion speed of this compound is the lowest among the low reactivity fuels tested (see Table 1).

Furthermore, lower pressure peak values were obtained when increasing the LRF content despite all tests were performed keeping a similar energy input. As stated in previous works [32,38], this was due to the inefficient combustion of the gaseous fuel located close to the chamber walls and far away from the liquid jets. No flame propagation throughout the very lean LRF/air mixtures is expected, the LRF burnt being that entraining in the fuel plumes. This was particularly noticeable at 600 °C, for which the amount of entrained LRF is smaller because of the shorter ignition delays. The higher fuel density at 535 °C (the
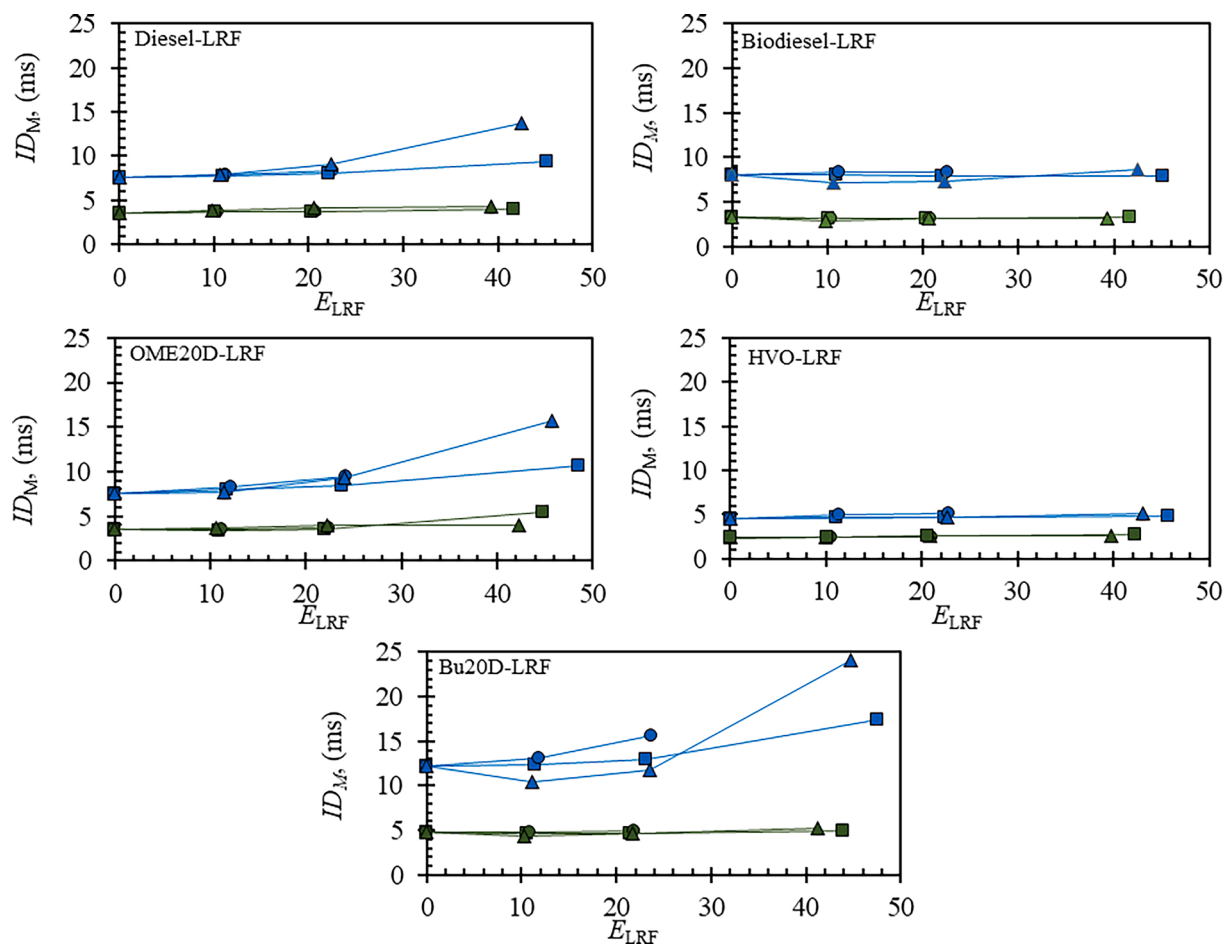
Fig. 4. Main ignition delay time for different replacements with H₂ (●), NH₃ (▲) and CH₄ (■) at $p_0 = 21$ bar and $T_0 = 535$ (blue) and 600 °C (green). (For interpretation of the references to color in this figure legend, the reader is referred to the web version of this article.)
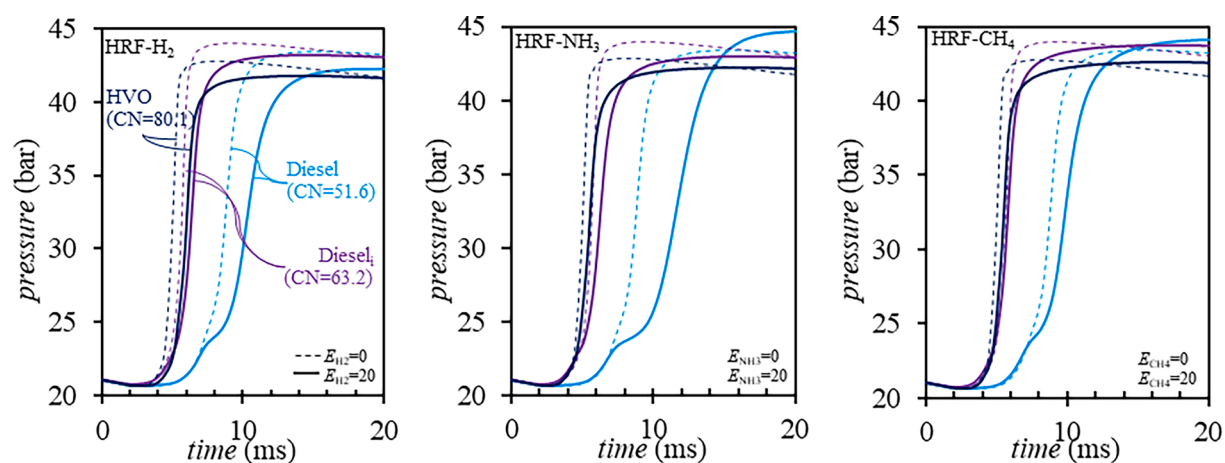

Fig. 5. Pressure traces for 20 % replacement of diesel, diesel₁ and HVO with H₂ (left), NH₃ (center), and CH₄ (right) at $p_0 = 21$ bar and $T_0 = 535$ °C (blue). (For interpretation of the references to color in this figure legend, the reader is referred to the web version of this article.)

injector is located inside the CVCC) masked the commented drop in the peak pressure since the energy provided by the HRF was slightly greater at this temperature (not the fuel mass but the volume was considered to achieve the desired energy content). The commented decrease in the pressure peak was less noticeable for hydrogen since its extreme mass diffusivity may enhance the entrainment into the liquid jets.

Fig. 4 shows the corresponding ID_M values derived from the pressure traces shown in Fig. 2. As reported in a previous work focused just on diesel fuel as HRF, the active radical sink effect of the LRF is the main reason for the observed longer ignition event under dual mode operation [39]. Moreover, other specific LRF kinetics effects should also be considered. NH₃, once the first H is abstracted, forms amino radicals (NH₂•), as reported by Manias et al. [40] using a kinetics analysis based on Computational Singular Perturbation. Similarly, CH₄ produces methyl radicals (CH₃•). While the latter transforms into methyl-peroxy radicals (CH₃—O—O•), which initiate the oxidation process, NH₂• is
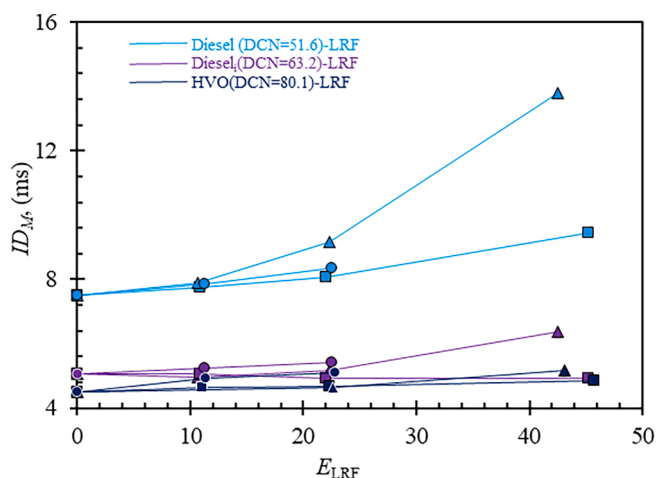
Fig. 6. Main ignition delay time for different replacements of diesel, diesel$_i$ and HVO with H$_2$ (●), NH$_3$ (▲) and CH$_4$ (■) at p_0 = 21 bar and T_0 = 535 °C.

not likely to react with O$_2$ to form the equivalent NH$_2$—O—O• but with O• atoms leading to aminooxy radicals (NH$_2$—O•). These latter radicals recombine to form stable hydrazine (N$_2$H$_4$), which slows down the chain-branching pathway. This particular effect of ammonia (the formation of stable intermediates) causes autoignition to be retarded to a greater extent when compared to hydrogen and methane.

As mentioned in the experimental section, additional tests including the improved diesel fuel have been carried out to elucidate the role of the HRF reactivity (quantified through the cetane number) on autoignition under dual mode. This fuel has been compared with the reference diesel fuel and HVO (all of them having a similar chemical structure). Fig. 5 (for E_{LRF} = 20 % as an example) and Fig. 6 show the pressure traces and the corresponding ID_M, respectively, at 535 °C. As observed, the higher the cetane number of the HRF the smaller the effect of the LRF. This is an interesting and practical result since it proves that the use of ignition improvers may be interesting not only for increasing the reactivity of a base fuel but also for extending dual-fuel CI combustion to the use of very autoignition-resistant but promising alternative LRF fuels (i.e., ammonia or methanol).

To check the role of the HRF chemical composition on autoignition, results for conventional diesel (DCN = 51.6), biodiesel (DCN = 52.5), OME20D (DCN = 53.1) and Bu20D$_i$ (DCN = 51.2) were compared, the latter resulting from adding 1.5 % by volume (15000 ppm) of 2-EHN to the blend, as described in section 2.2. All of them kept a very similar reactivity as derived from the DCN values. Although the DCN of the

OME20D was expected to be higher than that of diesel fuel, similar values were obtained. This result has been also reported in other works [41,42] for low OME contents (below 20 % by vol.), due to the higher heat of vaporization of OME when compared to diesel fuel, which counteracts its also higher reactivity at such concentrations.

As observed in Figs. 7 and 8 as well as in Fig. 2, biodiesel is less affected by the LRF type and content, while the ethers-containing fuel (OME20D) is the most sensitive. Because of biodiesel is a mixture of long-chain methyl esters, the proportion of methylene groups is higher than that of diesel. Since H atoms linked to these groups are more likely to be abstracted than those of primary C—H bonds [43], the latter more abundant in the diesel fuel because of its shorter C chain and the significant presence of branched structures (isoparaffins), the role of the LRF as active radicals sink is less pronounced for biodiesel. In addition, the allyl and bis-allyl groups of biodiesel molecules push the H-abstraction paths due to the low dissociation energy of the C—H adjacent to the carbon double bond [44]. The resonant effect produced by the double bond causes the BDE of the adjacent C—H bonds to decrease by approximately 10 and 20 kcal/mol, respectively, with respect to that of a C—H bond in an average alkane [45].

In contrast, OME20D was the fuel most affected by the LRF. While, as previously commented, the bond dissociation energy (BDE) of the primary C—H bonds is higher than that of the secondary ones for saturated hydrocarbons, the presence of several O atoms in the OMEx molecule
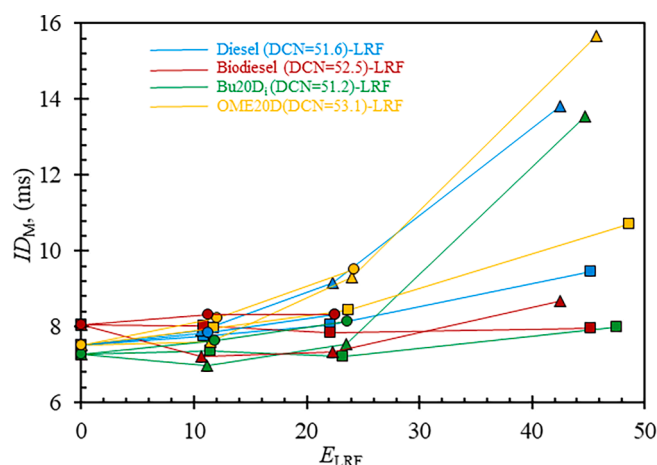

Fig. 8. Main ignition delay time for different replacements of diesel, biodiesel, Bu20D and OME20D with H$_2$ (●), NH$_3$ (▲) and CH$_4$ (■) at p_0 = 21 bar, T_0 = 535 °C.
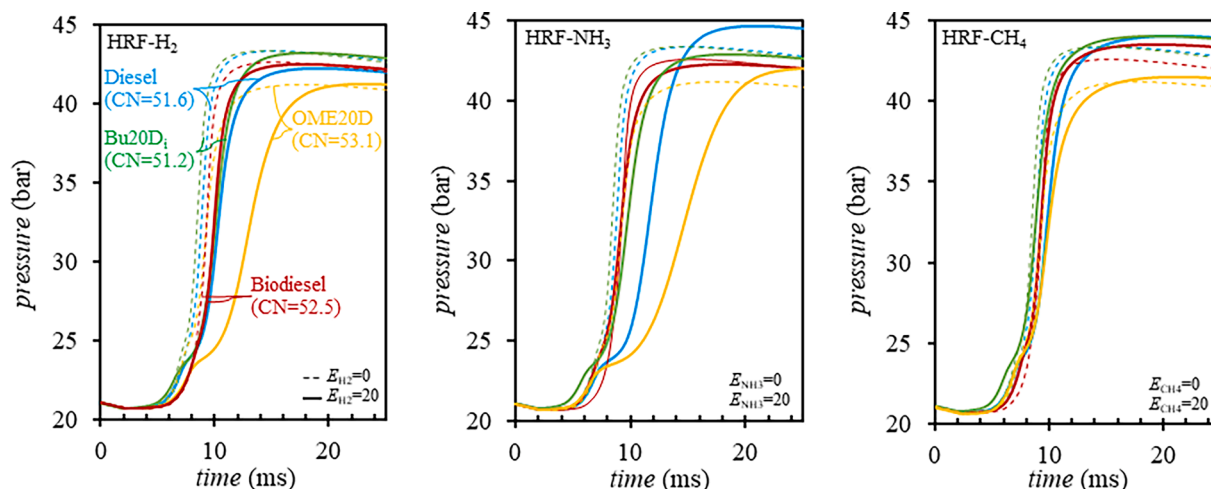

Fig. 7. Pressure traces for 20 % replacement of diesel, biodiesel, Bu20D and OME20D with H$_2$ (left), NH$_3$ (center), and CH$_4$ (right) at p_0 = 21 bar and T_0 = 535 °C.

causes an opposite trend [46,47]. Moreover, the BDE values are smaller and the difference in these values for both hydrogen abstraction sites is marginal when compared to that reported for hydrocarbons. Because of these aspects, a lower BDE of the C—H bonds and a more balanced branching ratio, the radical sink effect of the LRF was much more noticeable for the OME20D blend.

4. Conclusions

The need for increasing the share of sustainable diesel-type fuels in medium and heavy-duty CI engines, together with the potential of some H_2-derived fuels for reducing not only net CO_2 emissions but also other pollutant compounds, encourages the use of dual-fuel combustion modes combining both type of fuels. Dual-fuel operation also appears as a cost-effective technique for the retrofitting of current diesel engines looking for a higher sustainability, since most of the alternative liquid fuels must be blended with conventional diesel fuel (because of their poor physical and thermal-chemical properties), while most of the H_2-derived fuels cannot be used as pure in CI engines because of its extremely high autoignition resistance. This work analyses the auto-ignition behaviour (a key phenomenon governing performance and emissions of CI engines) of several advanced liquid fuels (HRFs) when operating under dual mode with H_2, CH_4 and NH_3 (LRFs), trying to isolate the effect of the reactivity of the HRF from that of its chemical structure (the latter leading to different reaction pathways). The study, which covers different replacements (by energy) of the HRF with the gaseous one (up to 40 %), has been performed under well controlled conditions in a constant volume combustion chamber. The main conclusions can be summarized as follows:

- While the occurrence of cool flames appears to be independent of the nature of the LRF and its energy ratio, the main ignition delay time considerably increases with the amount of LRF.
- Ammonia showed a more significant effect on the autoignition time than methane and hydrogen, not only due to its previously documented sink effect but also to the formation of stable intermediates (N_2H_4), the latter slowing down the chain-branching reactions.
- Tests carried out by using HRFs with different DCN but similar chemical structure revealed that the higher the reactivity of the HRF, the lower the influence of the LRF. This result suggests that the use of cetane improvers may be beneficial for extending dual-fuel operation towards LRFs with very poor autoignition properties.
- Regarding the effect of the liquid fuel chemical structure, biodiesel was the least affected by the presence of the LRF because of its elevated secondary/primary C—H ratio as well as the existence of allyl and bis-allyl groups, while the blend with OME_{3-5} (OME20D) was very sensitive to the LRF type and content due to both, the lower dissociation energy of its C—H bonds when compared to saturated hydrocarbons and its more balanced branching ratio.

Declaration of Competing Interest

The authors declare the following financial interests/personal relationships which may be considered as potential competing interests: [Juan J. Hernandez reports financial support was provided by Spain Ministry of Science and Innovation.].

Data availability

No data was used for the research described in the article.

Acknowledgements

Appendix A. Supplementary data

Supplementary data to this article can be found online at https://doi.org/10.1016/j.fuel.2023.127487.

References

[1] Chen H, He J, Zhong X. Engine combustion and emission fuelled with natural gas: a review. J Energy Inst 2019;92(4):1123–36.

[2] Papagiannakis RG, Hountalas DT, Rakopoulos CD. Theoretical study of the effects of pilot fuel quantity and its injection timing on the performance and emissions of a dual-fuel diesel engine. Energy Convers Manage 2007;48(11):2951–61.

[3] Yu X, Sandhu NS, Yang Z, Zheng M. Suitability of energy sources for automotive application – a review. Appl Energy 2020;271:115169.

[4] Pham Q, Park S, Agarwal A, Park S. Review of dual-fuel combustion in the compression-ignition engine: Spray, combustion, and emission. Energy 2022;250 (123778). https://doi.org/10.1016/j.energy.2022.123778.

[5] Liu H, Ma G, Hu B, Zheng Z, Yao M. Effects of port injection of hydrous ethanol on combustion and emission characteristics in dual-fuel reactivity controlled compression ignition (RCCI) mode. Energy 2018;145:592–602. https://doi.org/10.1016/j.energy.2017.12.089.

[6] Wei L, Geng P. A review on natural gas/diesel dual fuel combustion, emissions and performance. Fuel Process Technol 2016;142:264–78. https://doi.org/10.1016/j.fuproc.2015.09.018.

[7] Dimitriou P, Tsujimura T. A review of hydrogen as a compression ignition engine fuel. Int J Hydrogen Energy 2017;42(38):24470–86.

[8] Kumar R, Loganathan M, Gunasekaran E. Performance, emission and combustion characteristics of CI engine fuelled with diesel and hydrogen. Front Energy 2015;9: 486–94. https://doi.org/10.1007/s11708-015-0368-4.

[9] Ming T, Richter Rd, Dietrich Oeste F, Tulip R, Caillol S. A nature-based negative emissions technology able to remove atmospheric methane and other greenhouse gases. Atmos Pollut Res 2021;12(5):101035.

[10] Valera-Medina A, Amer-Hatem F, Azad AK, Dedoussi IC, Joannon MD, Fernandes RX, et al. Review on ammonia as a potential fuel: from synthesis to economics. Energy Fuels 2021;35(9):6964–7029. https://doi.org/10.1021/acs.energyfuels.0c03685.

[11] Kurien C, Mittal M. Review on the production and utilization of green ammonia as an alternate fuel in dual-fuel compression ignition engines. Energy Convers Manag 2022;251(114990). https://doi.org/10.1016/j.enconman.2021.114990.

[12] Mounaïm-Rousselle C, Brequigny P. Ammonia as fuel for low-carbon spark-ignition engines of tomorrow's passenger cars. Front Mech Eng 2020;8(70). https://doi.org/10.3389/fmech.2020.00070.

[13] Haghighat Shoar F, Najafi B, Mosavi A. Effects of triethylene glycol mono methyl ether (TGME) as a novel oxygenated additive on emission and performance of a dual-fuel diesel engine fueled with natural gas/biodiesel. Energy Rep 2021; 7:1172–89. https://doi.org/10.1016/j.egyr.2021.01.088.

[14] Tarabet R, Lounici MS, Loubar K, Khiari K, Bouguessa R, Tazerout M. Hydrogen supplemented natural gas effect on a DI diesel engine operating under dual fuel mode with a biodiesel pilot fuel. Int J Hydrogen Energy 2018;43(11):5961–71. https://doi.org/10.1016/j.ijhydene.2017.09.045.

[15] Official Journal of the European Union, Directive (EU) 2018/2001 of the European Parliament and of the Council of 11 December 2018 on the promotion of the use of energy from renewable sources. L 328, 82-209, 2018.

[16] T. Hartikka, M. Kuronen, U. Kiiski, Technical Performance of HVO (Hydrotreated Vegetable Oil) in Diesel Engines. SAE Technical Paper 2012; 2012-01-1585. https://doi.org/10.4271/2012-01-1585.

[17] Szeto W, Leung DYC. Is hydrotreated vegetable oil a superior substitute for fossil diesel? A comprehensive review on physicochemical properties, engine performance and emissions. Fuel 2022;327(125065). https://doi.org/10.1016/j.fuel.2022.125065.

[18] Ferraro F, Russo C, Schmitz R, Hasse C, Sirignano M. Experimental and numerical study on the effect of oxymethylene ether-3 (OME3) on soot particle formation. Fuel 2021;286–1(119353). https://doi.org/10.1016/j.fuel.2020.119353.

[19] Baranowski C, Bahmanpour A, Kröcher O. Catalytic synthesis of polyoxymethylene dimethyl ethers (OME): a review. Appl Catal B 2017;217:407–20. https://doi.org/10.1016/j.apcatb.2017.06.007.

[20] Pélerin D, Gaukel K, Härtl M, Jacob E, Wachtmeister G. Potentials to simplify the engine system using the alternative diesel fuels oxymethylene ether OME1 and OME3−6 on a heavy-duty engine. Fuel 2020;259(116231). https://doi.org/10.1016/j.fuel.2019.116231.

[21] Oestreich D, Lautenschütz L, Arnold U, Sauer J. Reaction kinetics and equilibrium parameters for the production of oxymethylene dimethyl ethers (OMEs) from methanol and formaldehyde. Chem Eng Sci 2017;163:92–104. https://doi.org/10.1016/j.ces.2016.12.037.

[22] Pastor J, García A, Micó C, Lewiski F. Simultaneous high-speed spectroscopy and 2-color pyrometry analysis in an optical compression ignition engine fueled with OMEX-diesel blends. Combust Flame 2021;230(111437). https://doi.org/10.1016/j.combustflame.2021.111437.

[23] Omari A, Heuser B, Pischinger S, Rüdinger C. Potential of long-chain oxymethylene ether and oxymethylene ether-diesel blends for ultra-low emission engines. Appl Energy 2019;239:1242–9. https://doi.org/10.1016/j.apenergy.2019.02.035.

[24] Lapuerta M, Hernández J, Fernández-Rodríguez D, Cova-Bonillo A. Autoignition of blends of n-butanol and ethanol with diesel or biodiesel fuels in a constant-volume combustion chamber. Energy 2017;118:613–21. https://doi.org/10.1016/j.energy.2016.10.090.

[25] Kiani D, Baltrusaitis J. Surface chemistry of hydroxyapa tite for sustainable n-butanol production from bio-ethanol. Chem Catalysis 2021;4(16):782–801. https://doi.org/10.1016/j.checat.2021.06.005.

[26] Veza I, Muhamad Said MF, Latiff ZA. Recent advances in butanol production by acetone-butanol-ethanol (ABE) fermentation. Biomass Bioenergy 2021;144 (105919). https://doi.org/10.1016/j.biombioe.2020.105919.

[27] Lumpp B, Rothe D, Pastötter C, Lämmermann R, Jacob E. Oxymethylene ethers as diesel fuel additives of the future. MTZ Worldw 2011;72:34–8. https://doi.org/10.1365/s38313-011-0027-z.

[28] Liu J, Liu Z, Wang L, Wang P, Sun P, Ma H, et al. Effects of PODE/Diesel blends on particulate matter emission and particle oxidation characteristics of a common-rail diesel engine. Fuel Process Technol 2021;212(106634). https://doi.org/10.1016/j.fuproc.2020.106634.

[29] Lapuerta M, Ramos Á, Barba J, Fernández-Rodríguez D. Cold- and warm-temperature emissions assessment of n-butanol blends in a Euro 6 vehicle. Appl Energy 2018;218:173–83. https://doi.org/10.1016/j.apenergy.2018.02.178.

[30] P. Linstrom, NIST Chemistry WebBook. NIST Standard Reference Database Number 69. NIST Office of Data and Informatics. 2021. [En línea]. Available: https://webbook.nist.gov/chemistry/. [Último acceso: 11 2021].

[31] Chai WS, Bao Y, Jin P, Tang G, Zhou L. A review on ammonia, ammonia-hydrogen and ammonia-methane fuels. Renew Sustain Energy Rev 2021;147(111254). https://doi.org/10.1016/j.rser.2021.111254.

[32] Hernández J, Cova-Bonillo A, Wu H, Barba J, Rodríguez-Fernández J. Low temperature autoignition of diesel fuel under dual operation with hydrogen and hydrogen-carriers. Energ Conver Manage 2022;258(15516). https://doi.org/10.1016/j.enconman.2022.115516.

[33] American Society for Testing and Materials, ASTM D7668-Standard Test Method for Determination of Derived Cetane Number (DCN) of Diesel Fuel Oils—Ignition Delay and Combustion Delay Using a Constant Volume Combustion Chamber Method. West Conshohocken, USA, 2014.

[34] Lapuerta M, Sanz-Argent J, Raine R. Heat release determination in a constant volume combustion chamber from the instantaneous cylinder pressure. Appl Therm Eng 2014;63(2):520–7. https://doi.org/10.1016/j.applthermaleng.2013.11.044.

[35] Lapuerta M, Sanz-Argent J, Raine R. Ignition characteristics of diesel fuel in a constant volume bomb under diesel-like conditions. Effect of the operation parameters. Energy Fuel 2014;28:5445–54. https://doi.org/10.1021/ef500535j.

[36] Ghosh P. Predicción del efecto de los mejoradores de cetano en los combustibles diésel. Energy Fuels 2008;22(2):1073–9. https://doi.org/10.1021/ef0701079.

[37] Kuszewski H. Effect of adding 2-ethylhexyl nitrate cetane improver on the autoignition properties of ethanol-diesel fuel blend - Investigation at various ambient gas temperatures. Fuel 2018;224:57–67. https://doi.org/10.1016/j.fuel.2018.03.084.

[38] Hernández JJ, Salvador JB, Cova-Bonillo A. Autoignition of diesel-like fuels under dual operation with H2. Adv Mech Eng 2019;11(6). https://doi.org/10.1177/1687814019856781. 168781401985678.

[39] Hernández J, Lapuerta M, Barba J. Separate effect of H2, CH4 and CO on diesel engine performance and emissions under partial diesel fuel replacement. Fuel 2016;165:173–84.

[40] Manias D, Patsatzis D, Kyritsis D, Goussis D. NH3 vs. CH4 autoignition: A comparison of chemical dynamics. Combust Theory Model 2021;25(6):1110–31. https://doi.org/10.1080/13647830.2021.1890835.

[41] Parravicini M, Barro C, Boulouchos K. Experimental characterization of GTL, HVO, and OME based alternative fuels for diesel engines. Fuel 2021;292(120177). https://doi.org/10.1016/j.fuel.2021.120177.

[42] Parravicini M, Barro C, Boulouchos K. Compensation for the differences in LHV of diesel-OME blends by using injector nozzles with different number of holes: Emissions and combustion. Fuel 2020;259(116166). https://doi.org/10.1016/j.fuel.2019.116166.

[43] Boot M, Tian M, Hensen E, Sarathy S. Impact of fuel molecular structure on autoignition behavior - Design rules for future high performance gasolines. Prog Energy Combust Sci 2017;60:1–25. https://doi.org/10.1016/j.pecs.2016.12.001.

[44] Mehl M, Vanhove G, Pitz WJ, Ranzi E. Oxidation and combustion of the n-hexene isomers: A wide range kinetic modeling study. Combust Flame 2008;155(4):756–72.

[45] Li X, Xu X, You X, Truhlar D. Benchmark Calculations for Bond Dissociation Enthalpies of Unsaturated Methyl Esters and the Bond Dissociation Enthalpies of Methyl Linolenate. Chem A Eur J 2016;120(23):4025–36. https://doi.org/10.1021/acs.jpca.6b02600.

[46] Fenard Y, Vanhove G. A Mini-Review on the Advances in the Kinetic Understanding of the Combustion of Linear and Cyclic Oxymethylene Ethers. Energy Fuels 2021;35(18):14325–42. https://doi.org/10.1021/acs.energyfuels.1c01924.

[47] Sun W, Wang G, Li S, Zhang R, Yang B, Yang J, et al. «Speciation and the laminar burning velocities of poly(oxymethylene) dimethyl ether 3 (POMDME3) flames: An experimental and modeling study. Proc Combust Inst 2017;36(1):1269–78. https://doi.org/10.1016/j.proci.2016.05.058.